British Journal of Pharmacology

DOI:10.1111/j.1476-5381.2011.01358.x
www.brjpharmacol.org

RESEARCH PAPER

PGE_2-EP_2 signalling in endothelium is activated by haemodynamic stress and induces cerebral aneurysm through an amplifying loop via NF-κB

T. Aoki[1,2], M. Nishimura[1], T. Matsuoka[2], K. Yamamoto[3], T. Furuyashiki[2], H. Kataoka[1], S. Kitaoka[2], R. Ishibashi[1], A. Ishibazawa[3], S. Miyamoto[1], R. Morishita[4], J. Ando[3], N. Hashimoto,[5] K. Nozaki[6] and S. Narumiya[2,7]

[1]*Department of Neurosurgery Kyoto University Graduate School of Medicine, Kyoto, Japan,* [2]*Department of Pharmacology, Kyoto University Graduate School of Medicine, Kyoto, Japan,* [3]*Department of Biomedical Engineering, Graduate School of Medicine, University of Tokyo, Tokyo, Japan,* [4]*Department of Clinical Gene Therapy, Osaka University Graduate School of Medicine, Osaka, Japan,* [5]*National Cardiovascular Center, Osaka, Japan,* [6]*Department of Neurosurgery, Shiga University of Medical Science, Shiga, Japan, and* [7]*Core Research for Evolutional Science and Technology (CREST), Japan Science and Technology Corporation, Tokyo, Japan*

Correspondence
Professor Shuh Narumiya, Department of Pharmacology, Kyoto University Graduate School of Medicine, Konoe-cho Yoshida, Sakyo-ku, Kyoto City, Kyoto, 606-8501 Japan. E-mail: snaru@mfour.med.kyoto-u.ac.jp

Keywords
cerebral aneurysm; inflammation; prostaglandin; EP_2; COX-2; NF-κB

Received
9 October 2010
Revised
23 December 2010
Accepted
10 January 2011

BACKGROUND AND PURPOSE

Cerebral aneurysm is a frequent cerebrovascular event and a major cause of fatal subarachnoid haemorrhage, but there is no medical treatment for this condition. Haemodynamic stress and, recently, chronic inflammation have been proposed as major causes of cerebral aneurysm. Nevertheless, links between haemodynamic stress and chronic inflammation remain ill-defined, and to clarify such links, we evaluated the effects of prostaglandin E_2 (PGE_2), a mediator of inflammation, on the formation of cerebral aneurysms.

EXPERIMENTAL APPROACH

Expression of COX and prostaglandin E synthase (PGES) and PGE receptors were examined in human and rodent cerebral aneurysm. The incidence, size and inflammation of cerebral aneurysms were evaluated in rats treated with COX-2 inhibitors and mice lacking each prostaglandin receptor. Effects of shear stress and PGE receptor signalling on expression of pro-inflammatory molecules were studied in primary cultures of human endothelial cells (ECs).

KEY RESULTS

COX-2, microsomal PGES-1 and prostaglandin E receptor 2 (EP_2) were induced in ECs in the walls of cerebral aneurysms. Shear stress applied to primary ECs induced COX-2 and EP_2. Inhibition or loss of COX-2 or EP_2 *in vivo* attenuated each other's expression, suppressed nuclear factor κB (NF-κB)-mediated chronic inflammation and reduced incidence of cerebral aneurysm. EP_2 stimulation in primary ECs induced NF-κB activation and expression of the chemokine (C-C motif) ligand 2, essential for cerebral aneurysm.

CONCLUSIONS AND IMPLICATIONS

These results suggest that shear stress activated PGE_2-EP_2 pathway in ECs and amplified chronic inflammation via NF-κB. We propose EP_2 as a therapeutic target in cerebral aneurysm.

Abbreviations

ACA, anterior cerebral artery; CA, cerebral aneurysm; COX, cyclooxygenase; EC, endothelial cell; EP_2, prostaglandin E receptor 2; IEL, internal elastic lamina; IL, interleukin; iNOS, inducible nitric oxide synthase; MMP, matrix metalloproteinase; NF-κB, nuclear factor κB; OA, olfactory artery; PGES, prostaglandin E synthase; *Ptger2*, EP_2 receptor gene; SMC, smooth muscle cell

Introduction

Subarachnoid haemorrhage is a serious cardiovascular event. It is fatal in 45% of patients within 30 days of onset, whereas 30% suffer from moderate to severe morbidity (van Gijn *et al.*, 2007). The main cause of subarachnoid haemorrhage is a rupture of a pre-existing cerebral aneurysm, which is seen in 1–5% of the general public (Wiebers *et al.*, 2003). Given this high prevalence and susceptibility to subarachnoid haemorrhage, treatment of cerebral aneurysm before rupture is important. Currently, there is no medical treatment that would directly interfere with cerebral aneurysm formation because the pathogenesis of these aneurysms remains unknown. In addition, surgical procedures for cerebral aneurysm have a risk of complication, even though it is low. Therefore, most patients are only given treatments to control some risk factors such as hypertension, rather than any direct treatment for the aneurysm itself.

To elucidate the molecular mechanisms of cerebral aneurysm formation, we established a rodent model of cerebral aneurysm (Hashimoto *et al.*, 1978; Morimoto *et al.*, 2002) through inducing haemodynamic stress at bifurcation sites of cerebral arteries. Haemodynamic force is considered to be a trigger of cerebral aneurysm formation by computational simulation (Alnaes *et al.*, 2007; Takeuchi and Karino, 2009), which demonstrated a high haemodynamic force at the site of cerebral aneurysms. Using the above model, we have been examining events leading to cerebral aneurysm formation. Recently, we have shown that chronic inflammation, mediated by nuclear factor κB (NF-κB) activation, increased the formation of cerebral aneurysms (Fukuda *et al.*, 2000, Sadamasa *et al.*, 2003; Moriwaki *et al.*, 2006; Aoki *et al.*, 2007a,b; Aoki and Nishimura, 2010). However, factors that link haemodynamic forces to NF-κB activation in the walls of cerebral aneurysms remain unclear, and thus, compounds aimed at medical treatment of these aneurysms are still to be discovered.

The prostanoids are a group of lipid mediators and are produced and released in response to various stimuli. Prostaglandin E_2 (PGE_2) is a prostanoid involved in various inflammatory diseases. PGE_2 is synthesized from arachidonic acid by sequential actions of two enzymes, cyclooxygenase (COX) and PGE synthase (PGES) (Tilley *et al.*, 2001). COX has two isoforms, COX-1 and COX-2, whereas PGES has three isoforms – microsomal PGES1 (mPGES1), mPGES2 and cytosolic PGES (cPGES) (Murakami *et al.*, 2002). Among them, COX-2 and mPGES1 are inducible enzymes in inflammatory events and are responsible for PGE_2 production in various inflammatory diseases. PGE_2 exerts its actions through a family of G protein-coupled receptors, EP_1 to EP_4 receptors (Narumiya *et al.*, 1999; Breyer *et al.*, 2001; Sugimoto and Narumiya, 2007; nomenclature follows Alexander *et al.*, 2009). Given that COX-2 is known to be induced in response to haemodynamic force and that PGE_2 elicits a variety of actions in inflammation, we hypothesized that PGE_2 signalling was involved in the pathogenesis of cerebral aneurysms and linked these haemodynamic forces with NF-κB activation (Topper *et al.*, 1996; Ogasawara *et al.*, 2001).

In the present study, we have examined PGE_2 production, expression of related enzymes and PGE receptor subtypes, and demonstrated that PGE_2 signalling activated NF-κB through EP_2 and triggers chronic inflammation in cerebral aneurysm walls. We suggest COX-2 and EP_2 as candidate drug targets against cerebral aneurysms.

Methods

Animals

All animal care and experimental use complied with the National Institutes of Health Guide for the Care and Use of Laboratory Animals and was approved by the Institutional Animal Care and Use Committee of Kyoto University Graduate School of Medicine. Sprague Dawley rats and C57BL/6NCrSlc mice were purchased from Japan SLC (Shizuoka, Japan). Mice lacking the gene for each PG receptor, that is *Ptger1*, *Ptger2*, *Ptger3*, *Ptger4*, *Ptgir* (also known as IP) or *Tbxa2r* (also known as TP), were generated, backcrossed and bred as previously described (Kobayashi and Narumiya, 2002). Animals were maintained on a light/dark cycle of 14 h/10 h with free access to chow and water. In total, 130 rats and 190 mice were used in the present study.

Rodent cerebral aneurysm models and histological analysis of cerebral aneurysms

To induce cerebral aneurysms, 7-week-old rats or mice were subjected to the ligation of the left carotid artery, and systemic hypertension was induced by salt overloading and the ligation of left renal artery under general anaesthesia following pentobarbital injection (50 $mg \cdot kg^{-1}$ i.p.), without any neuromuscular blocking agents. This procedure is designed to increase the haemodynamic stress on arterial walls of a bifurcation from the right carotid artery to the bifurcation site of the anterior cerebral artery (ACA) and olfactory artery (OA). Sham-operated animals were treated in the same manner except for ligation of the carotid arteries and the renal artery. Following initiation of the aneurysm model, animals were fed special chow containing 8% sodium chloride and 0.12% β-aminopropionitrile (Tokyo chemical industry, Tokyo, Japan), an inhibitor of lysyl oxidase that catalyzes the cross-linking of collagen and elastin. Induction of cerebral aneurysms at the right ACA–OA bifurcation was assessed in rats and mice at 3 and 5 months after the start of the procedures

described above respectively. In the histological analysis, rats and mice were perfused with 4% paraformaldehyde, and serial sections of cerebral aneurysm walls were made. Then, sections were subjected to Elastica van Gieson staining. Induced cerebral aneurysms were histologically defined as follows. Internal elastic lamina (IEL) disruption is a lesion without outward bulging of arterial walls. Advanced aneurysm is an outward bulging of the arterial wall with IEL fragmentation. Aneurysm size was calculated as a mean of the largest transverse diameter and the height of the aneurysmal dome. In some experiments, celecoxib, 4-[5-(4-methylphenyl)-3-(trifluoromethyl)-1H-pyrazol-1-yl] benzenesulfonamide, a selective COX-2 inhibitor and a generous gift from Pfizer (New York, NY, USA), was mixed in the chow and fed during the indicated period (150 $mg \cdot kg^{-1} \cdot day^{-1}$).

Measurement of PGE_2 in cerebral aneurysms

The right ACA–OA bifurcation was dissected, rapidly frozen in liquid nitrogen and pulverized. PGE_2 was extracted, and its content was measured by ELISA (Biotrak EIA system, GE Healthcare, Buckinghamshire, UK) according to the manufacturer's instructions. Prostanoid concentrations were normalized to the wet weight of the tissue.

RNA extraction and quantitative real-time polymerase chain reaction (RT-PCR)

At 1 or 3 months after the initiation of cerebral aneurysm, rats were killed as described above. To obtain enough RNA to detect EP_2 mRNA expression in RT-PCR analysis, total RNA was extracted from the left half of the anterior portion of the circle of Willis, which is composed of the cerebral aneurysm lesion and surrounding 'non-cerebral aneurysm' region, and converted into cDNA using RNeasy Fibrous Tissue Mini Kit and Sensiscript reverse transcriptase (Qiagen, Hilden, Germany). Quantitative RT-PCR was done with QuantiTect SYBR Green PCR Kit (Qiagen) and LightCycler quick system 330 (Roche, Basel, Switzerland). β-actin was used as an internal control. The primer sets used for rat samples were: 5′-gtccgtgaagatgcgctacc-3′ and 5′-ccacatttatggagatagtc-3′ for *Cox-1*, 5′-cggtggagaggtgtatcctc-3′ and 5′-ggagcacaacagagtg tgtg-3′ for *Cox-2*, forward 5′-gttcacccatcagtttcc-3′, reverse 5′-caagacacagcaggcatagg-3′ for *Ptger1*, forward 5′-taatggc caggagaatgagg-3′, reverse 5′-aggaccgcataccttcagc-3′ for *Ptger2*, forward 5′-cagtccgaacactgtcatgg-3′, reverse 5′-ctttcctgctgtg cattgg-3′ for *Ptger3*, forward 5′-gaagtaggcgtggttgatgg-3′, reverse 5′-cctactgggcacattgttgg-3′ for *Ptger4*, forward 5′-aggca tttgtgaggtgaagg-3′, reverse 5′-catgaaggctgaaccagagg-3′ for *mPges1*, forward 5′-gactgccctacaagcacagc-3′, reverse 5′-gatgc gacactcacacatcc-3′ for *mPges2*. The primer sets used for human cells were: 5′-cttcaatgagtaccgcaagagg-3′ and 5′-agtccagggtagaactccaacg-3′ for *Cox-1*, 5′-acaccctctat cactggcatcc-3′ and 5′-aacattcctaccaccagcaacc-3′ for *Cox-2*, forward 5′-tttgctgcactcttctctctgg-3′, reverse 5′-actgaaggga ccagaaagttcc-3′ for *mPges1*, forward 5′-aagtactggctca tgctcaacg-3′, reverse 5′-gtagtcaaaggacgccagagc-3′ for *mPges2*, forward 5′-agcttctttggacacttgc-3′, reverse 5′-atagcagccacctt cattcc-3′ for *CCL2* (also known as *Mcp-1)*. For quantification, the second derivate maximum method was used for crossing point determination, using LightCycler Software 3.3 (Roche).

Antibodies, immunohistochemistry, Western blot analysis and gelatin zymography

Primary antibodies used in this study are as follows: anti-COX-1 (SC-7950, SantaCruz Biotechnolgy, Santa Cruz, CA, USA), anti-COX-2 (SC-1747, SantaCruz Biotechnolgy), anti-EP_2 (101750, Cayman, Ann Arbor, MI, USA), anti-mPGES1 (160140, Cayman), anti-mPGES2 (160145, Cayman), anti-cPGES (10209, Cayman), anti-phospho-p65 NF-κB subunit (Ser536) (3033, Cell Signaling, Danvers, MA, USA) and anti-human CCL2 (MAB2791, R&D, Minneapolis, MN, USA). Immunohistochemistry, Western blot analysis and gelatin zymography were performed as previously described (Aoki *et al.*, 2007b; 2009b). Briefly, 1 or 3 months after cerebral aneurysm induction, all rats were deeply anaesthetized and perfused transcardially with 4% paraformaldehyde (immunohistochemistry) or phosphate-buffered saline (PBS) (Western blot analysis and gelatine zymography). For immunohistochemistry, the ACA–OA bifurcation was dissected and embedded in optimum cutting temperature compound. Thin sections (5 μm) were cut and mounted on silane-coated slides. After blocking with 5% donkey serum (Jackson ImmunoResearch, Baltimore, MD, USA), the sections were incubated with primary antibodies, followed by the incubation with fluorescence-labelled secondary antibodies (Jackson ImmunoResearch). Fluorescent images were acquired through a conventional epifluorescent microscope (BX51N-34-FL-1, Olympus, Tokyo, Japan). Whole cell lysate was extracted from the anterior portion of the circle of Willis, composed of cerebral aneurysm lesions and 'non-cerebral aneurysm' regions, using Complete Lysis M Kit (Roche). Although cerebral aneurysms were formed in the left side, it was necessary to pool tissues from both the left and the right sides to detect EP_2 reproducibly. As a result, the collected tissue included the tissue from the right side, which may have diluted or masked a change in EP_2 expression in cerebral aneurysm walls. A sample (15 μg) of the whole cell lysate was used for each assay. After sodium dodecyl sulphate polyacrylamide gel electrophoresis, separated proteins were transferred to polyvinylidene fluoride membranes (Hybond-P, GE Healthcare) and blocked with enhanced chemiluminescent (ECL) plus blocking agent (GE Healthcare). The membranes were then incubated with primary antibodies followed by incubation with horseradish peroxidase-conjugated anti-IgG antibody (GE Healthcare). The signal was detected by chemiluminescent reagent (ECL Plus Western Blotting Detection System, GE Healthcare). α-Tubulin served as an internal control. In gelatin zymography, whole cell lysate was applied to a Gelatin Zymo Electrophoresis Kit (Primary cell, Sapporo, Japan) according to the manufacturer's instructions. The gelatinolytic activity of each group was measured by densitometry and calculated as a ratio to that of the sham-operated group.

Human cerebral aneurysm samples were obtained with informed consent and approval of the ethical committee at Kyoto University from five patients with unruptured cerebral aneurysms during neurosurgical procedures. Control arterial walls were dissected from cadavers that had been preserved by freezing as quickly as possible after death to limit degenerative change (n = 3).

Primary cultures of endothelial cells from human carotid artery

Primary endothelial cells (ECs) from human carotid artery were purchased from Cell Applications (San Diego, CA, USA). Characteristics of these cells were confirmed to be compatible with those of ECs by morphological examination, Western blot analysis for von Willebrand factor, immunostaining for vascular endothelial-cadherin and uptake of acetyl low-density lipoprotein (LDL) (Supporting Information Figure S1A–D). In some experiments, ECs were incubated with selective agonists to each EP receptor subtype. Selective EP receptor agonists (EP_1: ONO-D1-004, Ki = 0.15 μM, EP_2: ONO-AE1-259, Ki = 0.003 μM, EP_3: ONO-AE-248, Ki = 0.0075 μM, EP_4: ONO-AE1-329, Ki = 0.0097 μM) were provided by Ono Pharmaceutical Co. Ltd (Osaka, Japan) (Sugimoto and Narumiya, 2007).

Loading shear stress

Primary ECs were cultured on gelatin-coated glass slides and were loaded with shear stress at 1.5 Pa (15 dyne·cm^2), which was equivalent to a stress experimentally proven to be loaded on cerebral aneurysm walls of rats *in vivo* (Nakatani *et al.*, 1991) and also frequently used in shear stress experiment (Inoue *et al.*, 2002), with a custom-made apparatus, as previously described (Yamamoto *et al.*, 2006). After 24 h of shear stress loading, cells were subjected to RT-PCR analysis or immunohistochemistry.

EP_2 receptor gene (Ptger2) knockdown by RNAi in ECs

Primary ECs were transfected with *Ptger2* siRNA (5′-caguauuacucuuacaagagu-3′ and 5′-ucuuguaagaguaauacugua-3′) or scrambled siRNA at 100 nM, which had been shown in preliminary studies to be effective in depleting *Ptger2* mRNA. From 72 h after the transfection, ECs were incubated with the EP_2 agonist (ONO-AE1-259) for 24 h and were then subjected to RT-PCR and Western blot analyses.

Primary culture of smooth muscle cells

Primary culture of smooth muscle cells (SMCs) from rat cerebral arteries was established as previously described (Ishibashi *et al.*, 2010). Briefly, the whole circle of Willis was isolated from rats under deep anaesthesia. Dissected tissue was cut into small pieces and incubated with collagenase and elastase under gentle shaking. Dispersed cells were collected and incubated in a fibronectin-coated dish with medium containing epithelial growth factor, fibroblast growth factor, insulin and fetal bovine serum.

NF-κB decoy oligodeoxynucleotide treatment

NF-κB decoy oligodeoxynucleotide (ODN) and scrambled ODN were synthesized as previously described (Morishita *et al.*, 2004). In rat cerebral aneurysm experiments, 40 μg of decoy ODN dissolved in PBS was injected into the cerebrospinal fluid space from the foramen magnum, as previously described (Aoki *et al.*, 2007b). In primary EC experiments, decoy ODN or scrambled ODN (400 nM) was transfected. At 4 h after the transfection, treatment with the EP_2 agonist (ONO-AE1-259) was initiated.

Statistical analysis

Data are shown in mean ± SEM. Differences between two groups were statistically examined using Mann–Whitney test. Statistical comparisons among more than two groups were conducted using Kruskal–Wallis test followed by *post hoc* Dunn's test. The cerebral aneurysm incidence across groups was statistically compared with Fisher's exact test.

Results

Induction of COX-2–PGE_2–EP_2 signalling in cerebral aneurysm walls

We first examined the cerebral artery of patients with cerebral aneurysms and found extensive expression of COX-2 in the cerebral aneurysm walls but not in other regions (Figure 1A; Supporting Information Figure S2A). To further confirm the involvement and actions of PGs in cerebral aneurysm development, we used the rodent model, in which rats were subjected to unilateral carotid ligation and systemic hypertension by salt overloading (Aoki *et al.*, 2007b). After 3 months, cerebral aneurysm develops at the contralateral arterial bifurcation site in the circle of Willis, where cerebral aneurysm is also observed in most human patients (Wiebers *et al.*, 2003; van Gijn *et al.*, 2007) (Figure 1B). We found that, for the two COX isoforms, COX-2 but not COX-1 was induced at both mRNA and protein levels in cerebral arteries during cerebral aneurysm induction, a finding similar to that observed in walls of human cerebral aneurysm (Figure 1C and D; Supporting Information Figure S3A–C). In addition, mPGES1, a major inducible form of PGES, but not mPGES2, was induced in cerebral arteries (Figure 1C and D; Supporting Information Figure S3D). Consistent with the induction of this enzyme, the amount of PGE_2 significantly increased in cerebral aneurysm walls compared with that found in the sham-operated artery (Figure 1E). PGE_2 primarily binds to G protein-coupled receptors, EP_1–EP_4, for its action (Sugimoto and Narumiya, 2007). We analysed expression of EP receptor subtypes and found that only EP_2 expression was induced at cerebral aneurysms (Figure 1F; Supporting Information Figure S4), suggesting that PGE_2 produced by the COX-2–mPGES1 pathway acted on EP_2. Immunostaining revealed that expression of COX-2, mPGES1 and EP_2 was predominantly present in the EC layer of cerebral aneurysm walls at 2 weeks, the early stage of cerebral aneurysm formation (Figure 1G). At 3 months, when cerebral aneurysm formation was apparent, COX-2 and mPGES1 expression was extended to other regions such as SMCs in the aneurysm walls, suggesting augmentation of the production of PGE_2 at a later stage (Figure 1G).

These results indicated that hypertensive stress acts first on ECs at the prospective site of a cerebral aneurysm in the cerebral artery and induces COX-2, mPGES1 and EP_2. To confirm this possibility, we used primary culture of ECs from human carotid artery (Supporting Information Figure S1A–D), exposed them to shear stress *in vitro* and examined the effect of shear stress on the expression of these molecules. Shear stress induced COX-2 mRNA and protein in these cells (Figure 1H; Supporting Information Figure S1E and F). Shear stress further significantly elevated *Ptger2* mRNA in these cells

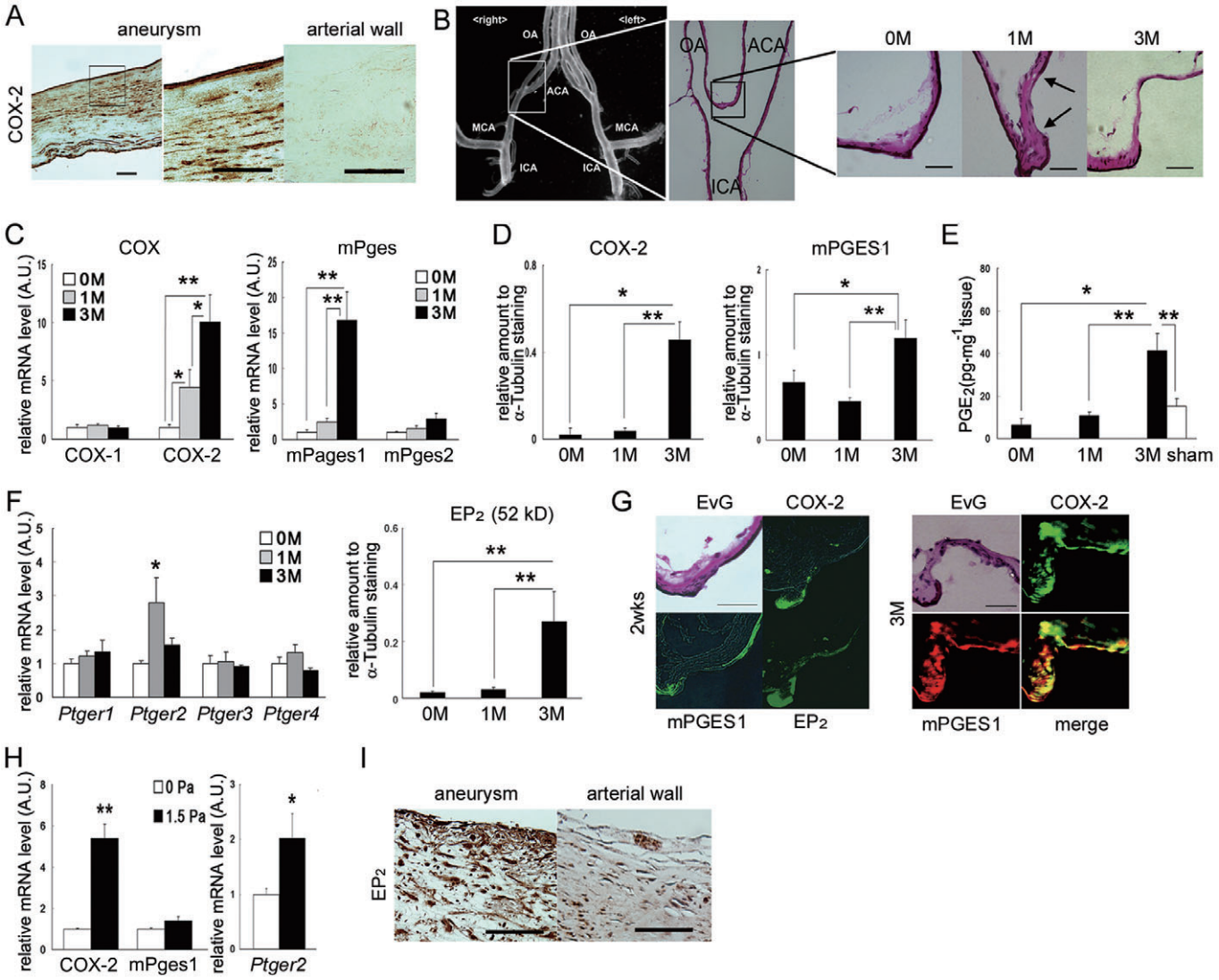

Figure 1

PGE_2-EP_2 signalling was induced during cerebral aneurysm formation. (A) COX-2 expression in cerebral aneurysm walls of human patients (left, middle) and the wall of a control cerebral artery (right). Bar = 50 μm. (B) Location and time course of cerebral aneurysm induction in the rat model. The circle of Willis of the rat is shown in the left panel. The boxed region shows the ACA–OA bifurcation where cerebral aneurysm was induced. Microscopic images, stained with Elastica van Gieson, of dissected arterial walls of this region are shown in the right panels. Arrows show the boundaries of disruption of internal elastic lamina. OA: olfactory artery. ACA, MCA: anterior or middle cerebral artery. ICA: internal carotid artery. 0,1 or 3 M: before and at 1 or 3 months after induction of cerebral aneurysm. Bar = 20 μm. (C, D) RT-PCR (C, $n = 6$) and Western blot analysis (D, $n = 5$) for expression of isoforms of COX and PGES in rat cerebral artery during the formation of cerebral aneurysm. Data represent mean ± SEM. $^*P < 0.05$, $^{**}P < 0.01$. (E) PGE_2 content measured by ELISA in the ACA–OA bifurcation of rats after induction of cerebral aneurysm ($n = 5$). Data represent mean ± SEM. $^*P < 0.05$, $^{**}P < 0.01$. (F) RT-PCR ($n = 6$) and Western blot analysis ($n = 5$) for expression of PGE receptor (EP) subtypes in rat cerebral artery during the formation of cerebral aneurysm. Data represent mean ± SEM. $^*P < 0.05$ compared with the level before induction of cerebral aneurysm (0 M). $^{**}P < 0.01$. (G) Immunostaining for COX-2, mPGES1 and EP_2 in cerebral aneurysm walls during cerebral aneurysm formation. The cerebral aneurysm walls of rats 2 weeks (2 wks) or 3 months (3 M) after induction of cerebral aneurysm were dissected and stained. EvG: Elastica van Gieson staining. The endothelial cell layer is defined as a cell layer outside the internal elastic lamina. Bar = 20 μm. (H) RT-PCR analysis for *Cox-2* and *Ptger2* mRNA expression in cultured endothelial cells exposed to shear stress ($n = 7$). Data represent mean ± SEM. $^*P < 0.05$, $^{**}P < 0.01$. (I) Immunostaining for EP_2 in the cerebral aneurysm walls of human patients (left) and the corresponding region of control subjects (right). Bar = 50 μm.

(Figure 1H). Consistent with these findings, we noted strong expression of EP_2 in the cerebral aneurysm walls but not in other cerebral arterial regions of human patients (Figure 1I; Supporting Information Figure S2B). These data support the proposal that shear stress induced PGE_2-EP_2 receptor signalling in ECs at the site of cerebral aneurysm formation and suggest that PGE_2-EP_2 signalling could link hypertensive stress to the formation of cerebral aneurysms.

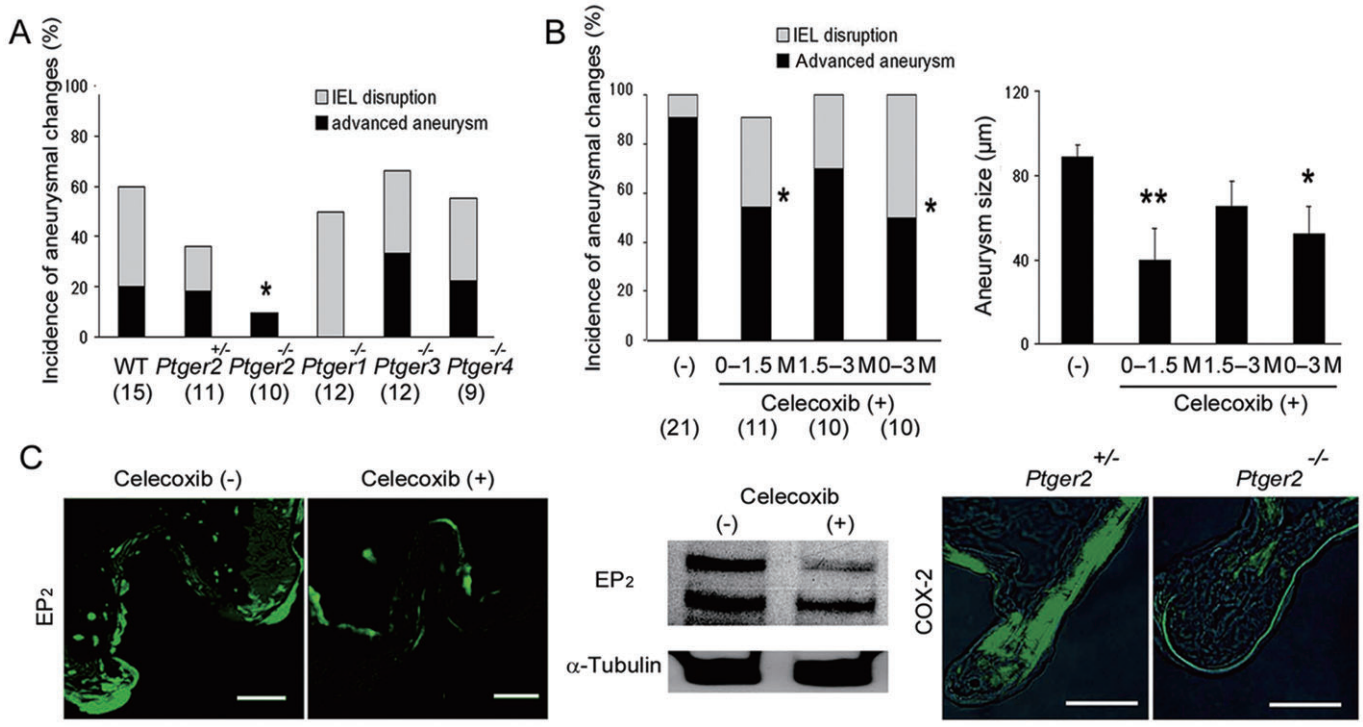

Figure 2

Effects of EP_2 deletion (knockout) and COX-2 inhibition on cerebral aneurysm formation. (A) Induction of cerebral aneurysm in mice lacking each EP receptor subtype. Aneurysmal changes were histologically assessed at 5 months after induction of cerebral aneurysm. Numbers of animals are shown in parentheses. *$P < 0.05$ compared with the incidence in wild-type mice (WT). (B) Effects of COX-2 inhibition. Rats were treated with or without celecoxib during the whole experimental period (0–3 months) or its former (0–1.5 months) or latter (1.5–3 months) half. Aneurysmal changes (left) and the size of aneurysm (right) were histologically assessed and are shown for each group. The number of animals is shown in parentheses under each bar. M, month. Data represent mean ± SEM. *$P < 0.05$, **$P < 0.01$. (C) Positive feedback induction between COX-2 and EP_2. Rats were treated with or without celecoxib for 3 months and examined for expression of EP_2 by immunostaining (left) and Western blot analyses (middle). *Ptger2*-heterozygous (*Ptger2*$^{+/-}$) and *Ptger2*-knockout (*Ptger2*$^{-/-}$) mice were subjected to induction of cerebral aneurysm for 5 months and examined for expression of COX-2 by immunostaining (right). Bar = 20 μm.

Involvement of COX-2-EP_2 signalling in the pathogenesis of cerebral aneurysm formation

To examine any causal relationship between EP receptors and the development of cerebral aneurysms, we subjected mice deficient in each EP receptor subtype (Kobayashi and Narumiya, 2002; Aoki *et al.*, 2007b) to the procedure for inducing cerebral aneurysms. Consistent with the altered expression of EP_2 in cerebral aneurysm walls (Figure 1F and I), cerebral aneurysm formation was almost absent in *Ptger2*-deficient mice, but not in the other three knockout strains (Figure 2A). *Ptger2* heterozygous mice showed intermediate incidence of cerebral aneurysm formation between wild-type and *Ptger2*-deficient mice, suggesting the gene dosage effect of *Ptger2*. *Ptger2*-deficient mice did not show any apparent abnormality in the structure of the circle of Willis or of the systemic blood pressure (Supporting Information Figure S5). In addition, mice deficient in the receptors for thromboxane (TX) A_2 and PGI_2, prostanoids involved in atherosclerosis (Kobayashi *et al.*, 2004), developed cerebral aneurysms similarly to wild-type mice (Supporting Information Figure S6).

To confirm the involvement of the PGE_2-EP_2 signalling in the pathogenesis of cerebral aneurysm, we administered celecoxib, a selective COX-2 inhibitor (Everts *et al.*, 2000), to rats subjected to cerebral aneurysm induction. Celecoxib, given orally for 3 months, significantly reduced the incidence of advanced aneurysm (Figure 2B) without affecting the systemic blood pressure (Supporting Information Figure S7A). Note that the celecoxib treatment during the earlier half (0–1.5 months), but not during the latter half (1.5–3.0 months), significantly reduced both the incidence and the size of cerebral aneurysm to levels similar to those found in the whole-period treatment (Figure 2B). Given the expression of COX-2, mPGES1 and EP_2 in ECs at the early stage of cerebral aneurysm induction (Figure 1G), these data suggest that PGE_2-EP_2 signalling acts primarily in ECs at the initial stage and triggers cerebral aneurysm formation. We next wondered whether COX-2 and EP_2 formed a positive feedback loop because each mutually affects the expression of the other under various physiological and pathological conditions (Sonoshita *et al.*, 2001). Indeed, the celecoxib treatment suppressed EP_2 expression in cerebral aneurysm walls (Figure 2C). Conversely, COX-2 expression in cerebral aneurysm walls was suppressed in *Ptger2*-deficient mice (Figure 2C). Thus, a positive feedback between COX-2 and EP_2 also operates in cerebral aneurysm walls.

Regulation of chronic inflammation in cerebral aneurysm walls via COX-2-EP_2 signalling in vivo

Earlier studies have demonstrated that chronic inflammation characterized by infiltration of macrophages was present in the cerebral aneurysm wall and played a causative role in cerebral aneurysm formation (Chyatte *et al.*, 1999; Fukuda *et al.*, 2000; Moriwaki *et al.*, 2006; Aoki *et al.*, 2007a,b; 2009b). In our present experiments, we noted that macrophage infiltration was suppressed in cerebral aneurysm walls of both *Ptger2*-deficient mice and rats treated with celecoxib (Figure 3A; Supporting Information Figure S7B). As NF-κB is critical for the transcription of various pro-inflammatory mediators in cerebral aneurysm lesions (Aoki *et al.*, 2007b), we next examined the effects of EP_2 deficiency or COX-2 inhibition on the phosphorylation of NF-κB p65 subunit and expressions of downstream molecules, such as the chemokine CCL2, interleukin (IL)-1β, inducible nitric oxide synthase (iNOS) and matrix metalloproteinase (MMP)-2 (Fukuda *et al.*, 2000; Sadamasa *et al.* 2003; Moriwaki *et al.*, 2006; Aoki *et al.*, 2007a,b; 2008a; 2009b). EP_2 deficiency significantly suppressed NF-κB activation and down-regulated induction of all of these molecules as shown by both immunostaining and Western blot analyses (Figure 3B and C). The celecoxib treatment also suppressed NF-κB activation and the induction of MMP-2, CCL2 and IL-1β (Supporting Information Figure S7C, D and F). We also visualized MMP-2 activity using gel zymography and confirmed the inhibitory effect of celecoxib (Supporting Information Figure S7E). Consistent with the fact that COX-2 is transcriptionally regulated by NF-κB activation (Schmedtje *et al.*, 1997), NF-κB activation and COX-2 expression were co-localized in cerebral aneurysm walls of the rats (Supporting Information Figure S7G). Furthermore, NF-κB inhibition by decoy ODN, a specific inhibitor of NF-κB transcriptional activity (Morishita *et al.*, 2004), suppressed COX-2 expression in cerebral aneurysm walls, suggesting the presence of a positive feedback loop between COX-2 and NF-κB (Supporting Information Figure S7H) via EP_2 (see below). These results, combined together, suggest that shear stress-induced PGE_2-EP_2 receptor signalling activates NF-κB in ECs at an early stage and contributes to chronic inflammation in arterial walls for cerebral aneurysm formation.

Regulation of NF-κB mediated CCL2 expression in ECs via PGE_2-EP_2 signalling in vitro

Given that NF-κB is activated first in ECs and then in various cell component in cerebral aneurysm walls (Aoki *et al.*, 2007b) and that the inhibition of PGE_2-EP_2 signalling suppressed NF-κB activation (Figure 3; Supporting Information Figure S7), we hypothesized that EP_2-mediated NF-κB activation induced CCL2 expression in ECs to trigger cerebral aneurysm formation. To corroborate this hypothesis, we again used primary culture of ECs from human carotid artery and examined the effect of the EP_2 agonist (ONO-AE1-259) on the phosphorylation of NF-κB and expression of CCL2. We found that PGE_2 significantly induced CCL2 in ECs (Supporting Information Figure S8A, B). ONO-AE1-259, but not agonists for other EP receptor subtypes, mimicked this increase in CCL2 (Figure 4A and B). We then examined whether NF-κB is involved in EP_2-mediated induction of CCL2. ONO-AE1-259 induced NF-κB phosphorylation in these cells (Figure 4B), which was blocked by RNAi for *Ptger2*, the gene coding for EP_2 (Figure 4C; Supporting Information Figure S8C–E). *Ptger2* depletion by RNAi also blocked the *CCL2* increase (Figure 4C). We also found that NF-κB decoy ODN blocked the EP_2-mediated *CCL2* induction (Figure 4D). Thus, EP_2 receptor stimulation induced CCL2 via an NF-κB-dependent pathway in primary ECs. We further examined the effect of EP receptor agonists on the expression of pro-inflammatory mediators in primary SMCs from rat cerebral arteries (Ishibashi *et al.*, 2010) because EP_2 receptors are also expressed in SMCs at the late stage of cerebral aneurysm formation and cerebral aneurysm walls of human patients (Figure 1G and I; Supporting Information Figure S2B). ONO-AE1-259, but not agonists of other EP receptor subtypes, induced the expression of *Il-1β* and *iNos* (Fukuda *et al.*, 2000; Sadamasa *et al.*, 2003; Moriwaki *et al.*, 2006) in these cells (Supporting Information Figure S9). These data suggest that PGE_2-EP_2 signalling in EC and SMC is involved in the inflammation at distinct stages of cerebral aneurysm formation.

Discussion

In this study, we have presented several lines of evidence that PGE_2-EP_2 signalling functions as a link between haemodynamic stress and cerebral aneurysm formation through the activation of NF-κB and evokes chronic inflammation in rodent models of cerebral aneurysm. We have further provided evidence that this mechanism also operates in human patients. Recent analyses on samples from patients with cerebral aneurysm have strongly implicated chronic inflammation in the pathogenesis of this condition (Chyatte *et al.*, 1999; Takagi *et al.*, 2002; Jayaraman *et al.* 2005) and various findings in rodent cerebral aneurysm models support this notion (Aoki *et al.*, 2007b; 2009b; Aoki and Nishimura, 2010). Meanwhile, based on the findings that mechanical force is high at the site of cerebral aneurysm formation and that increased shear stress by surgical procedures in dogs induces pathological changes resembling cerebral aneurysm, the mechanical force exerted by blood flow (shear stress) has been proposed to be a cause for cerebral aneurysm formation (Hashimoto *et al.*, 1980; Nakatani *et al.*, 1991; Meng *et al.*, 2007; Takeuchi and Karino, 2009). However, how haemodynamic stress leads to chronic inflammation has thus far remained unknown. Here, we have further disclosed that, once shear stress triggers PGE_2-EP_2 signalling, it amplifies the inflammatory processes through a positive feedback loop containing EP_2, NF-κB and COX-2. Therefore, it appears that inflammation in cerebral aneurysm walls is boosted and maintained by a pathway of COX-2–PGE_2-EP_2 NF-κB signalling, resulting in cerebral aneurysm formation (Figure 5).

Shear stress and PGE_2 signalling have also been suggested to be involved in the pathogenesis of aortic aneurysms (Holmes *et al.*, 1997; Miralles *et al.*, 1999; King *et al.* 2006). However, previous studies suggest that the underlying pathogenesis of aortic aneurysms and cerebral aneurysms is different. Epidemiological studies have shown that the risk of

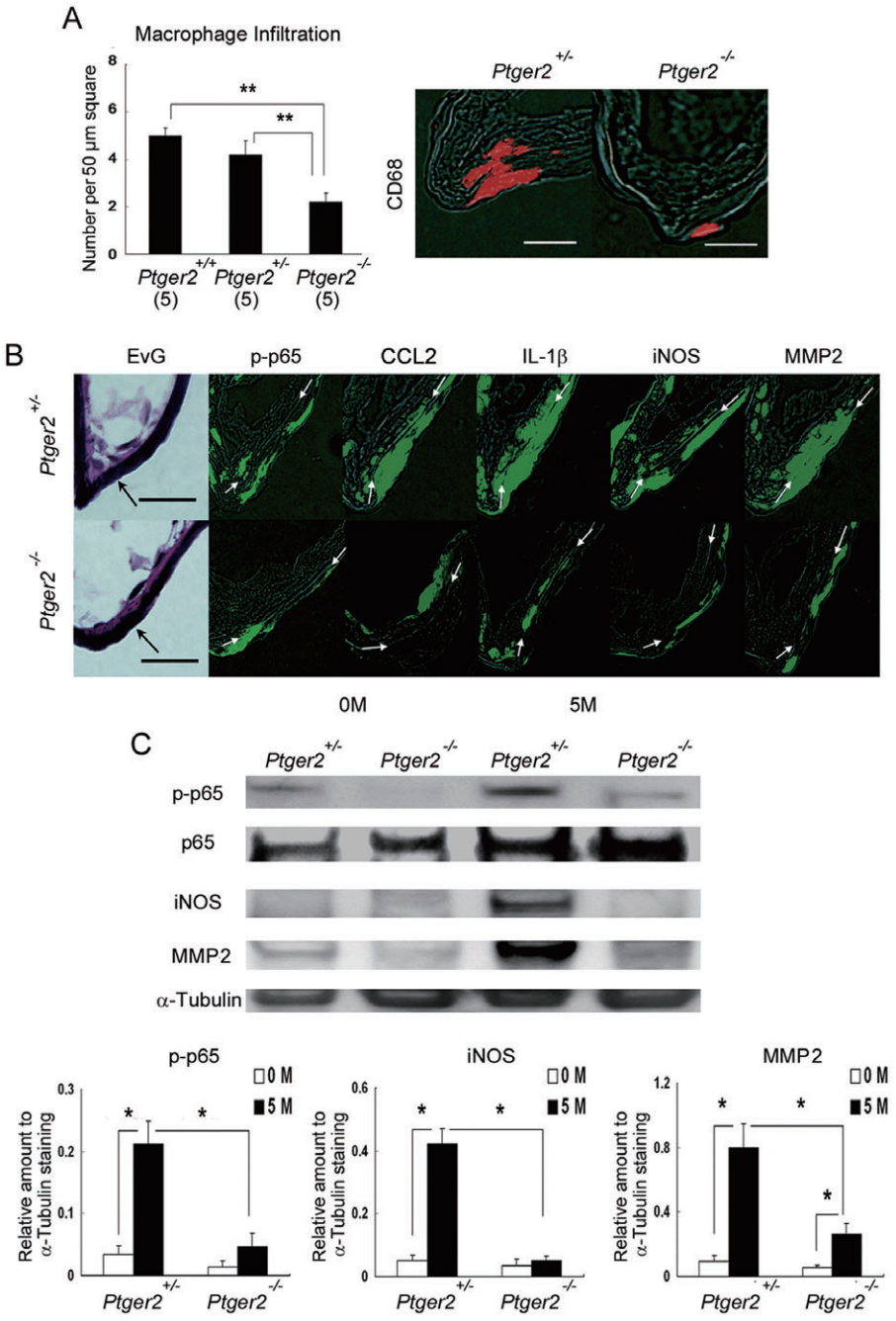

Figure 3

EP_2 signalling mediates chronic inflammation in cerebral aneurysm walls. (A) Effects of EP_2 deficiency on macrophage infiltration in cerebral aneurysm walls. The number of CD68-positive macrophages was determined in immunostained sections. The number of animals is shown in parentheses under each bar. Data represent mean ± SEM. $^{**}P < 0.01$. Representative images are shown in the right panel. Bar = 20 μm. (B) Immunostaining for pro-inflammatory mediators in walls of cerebral aneurysms in littermates of *Ptger2* heterozygous (*Ptger2*$^{+/-}$) and *Ptger2*-deficient (*Ptger2*$^{-/-}$) mice. Black arrows in Elastica van Gieson (EvG) staining (left) indicate the centre of the cerebral aneurysm or its corresponding position. White arrows indicate the internal elastic lamina of arterial walls. Bar = 20 μm. p-p65: phosphorylated NF-κB p65 subunit. (C) Effect of EP_2 deficiency on NF-κB activation and expression of pro-inflammatory mediators in cerebral arteries. Representative images of Western blot analyses are shown in the upper panels and the quantification by densitometric analysis is shown in the lower panel ($n = 5$). α-Tubulin was used as an internal control. 0 or 5 M: before and at 5 months after induction of cerebral aneurysm. Data represent mean ± SEM. $^{*}P < 0.05$.

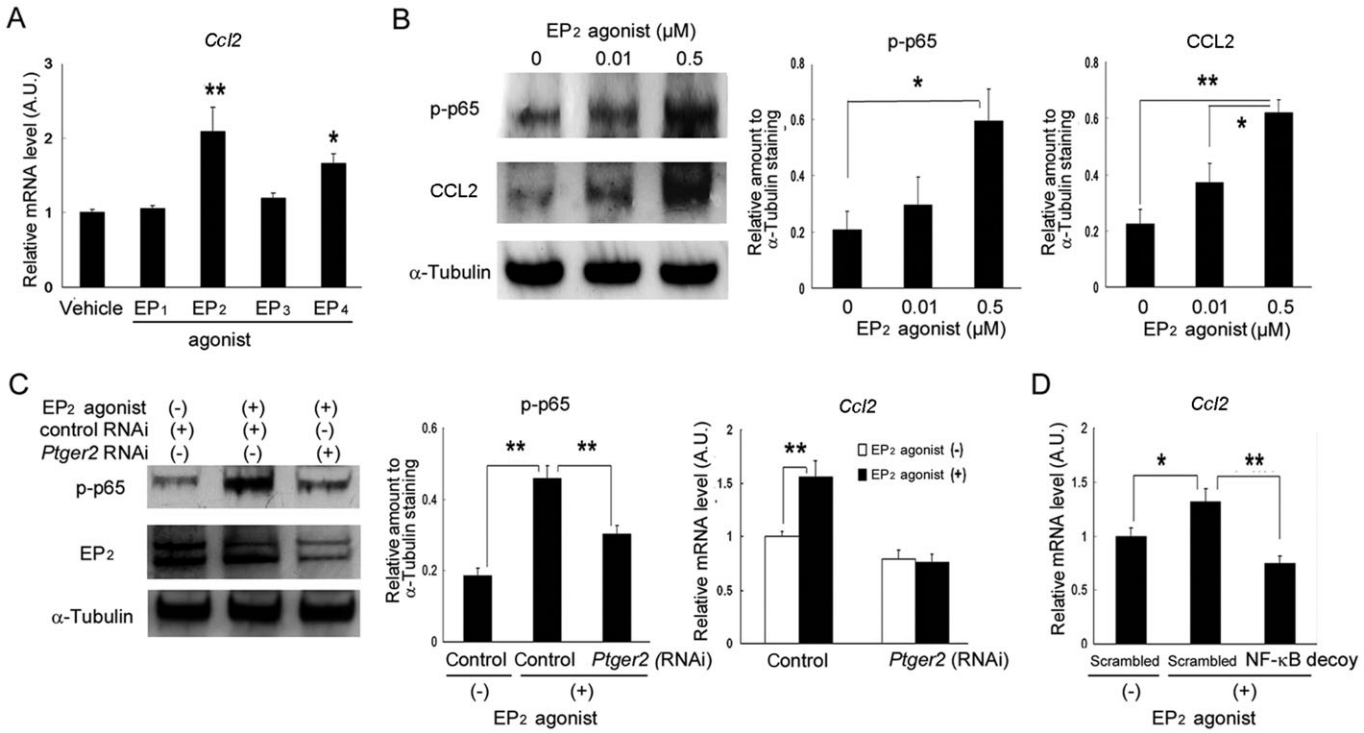

Figure 4

Induction of CCL2 expression by EP$_2$ stimulation via NF-κB pathway in ECs. (A) Effects of EP agonists on the mRNA level of *CCL2* in primary ECs from human carotid artery (EP$_1$ agonist; ONO-D1-004, EP$_2$ agonist; ONO-AE1-259, EP$_3$ agonist; ONO-AE-248, EP$_4$ agonist; ONO-AE1-329). After 24 h stimulation with the respective receptor agonists (0.5 μM), mRNA levels of *CCL2* were determined by RT-PCR ($n = 6$). Data represent mean ± SEM. *$P < 0.05$, **$P < 0.01$. (B) Effects of ONO-AE1-259, an EP$_2$ agonist, on phosphorylation of p65 subunit of NF-κB (p-p65) and CCL2 protein. The left panel shows representative images of Western blot analyses. Middle and right panels show the quantification by the densitometric analyses of phospho-p65 signals (middle) and CCL2 signals (right), respectively ($n = 5$). Data represent mean ± s,e,mean. *$P < 0.05$. **$P < 0.01$. (C) Effects of *Ptger2* depletion by RNAi on NF-κB phosphorylation and CCL2 expression induced by ONO-AE1-259. The left panel shows representative phosphorylated p65 subunit (p-p65) and EP$_2$ signals in Western blot analyses under the indicated conditions. The middle panel shows quantification by the densitometric analyses of phosphorylated-p65 signals ($n = 5$). The right panel shows mRNA levels of *CCL2* from ECs pretreated with siRNA for *Ptger2* or control siRNA without or with subsequent EP$_2$ stimulation ($n = 6$). Data represent mean ± SEM. **$P < 0.01$. (D) Effect of NF-κB inhibition by decoy oligodeoxynucleotide on EP$_2$-induced *CCL2* expression ($n = 6$). Data represent mean ± SEM. *$P < 0.05$, **$P < 0.01$.

cerebral aneurysm and aortic aneurysm are gender dependent as the relative risk of cerebral aneurysm is 1.6 in females (Linn *et al.*, 1996) while that of aortic aneurysm is 3.96 in males (Cornuz *et al.*, 2004). Atherosclerosis is now understood to be an inflammatory disease of the arteries. It has been accepted that aortic aneurysm occurs as a consequence of aortic degeneration by atherosclerosis. Hypercholesterolaemia, a major risk factor for atherosclerosis, also increases the incidence of aortic aneurysm, but not that of cerebral aneurysm (Cornuz *et al.*, 2004; Feigin *et al.*, 2005; van Gijn *et al.*, 2007). Consistent with these findings, hypercholesterolaemia induced by apolipoprotein E deficiency in mice, which causes atherosclerosis, does not increase the incidence of cerebral aneurysm (Aoki *et al.*, 2008c). Moreover, we found that PGI$_2$-IP and TXA$_2$-TP signalling, which suppress and facilitate atherosclerosis, respectively, failed to influence cerebral aneurysm formation (Supporting Information Figure S6). Furthermore, previous studies have implicated EP$_4$ and not EP$_2$ in the pathogenesis of aortic aneurysm (Bayston *et al.*, 2003). Therefore, it seems that different PGE receptor subtypes contribute to the formation of cerebral and aortic aneurysms.

Currently, there is no medical treatment for cerebral aneurysm except for the treatment of risk factors. From our present findings, COX-2 inhibition would be one option for cerebral aneurysm treatment as demonstrated in the rat experiments. However, the clinical use of COX-2 inhibitors for cerebral aneurysm has not been reported to date. We are currently performing a case-control study for evaluating the preventive effect of 3-hydroxy-3-methylglutaryl-coenzyme A reductase inhibitors (statins) on cerebral aneurysm rupture (subarachnoid haemorrhage-statin study). Statins have an anti-NF-κB activity through a pleiotropic effect (Liao and Laufs, 2005) and we have previously reported the preventive effect of statins on cerebral aneurysm formation in rat models (Aoki *et al.*, 2008b; Aoki *et al.* 2009a). Our clinical study also allows us to examine effects of other drugs on cerebral aneurysm rupture. In this survey, we have found that the administration of non-steroidal anti-inflammatory drugs (NSAIDs)

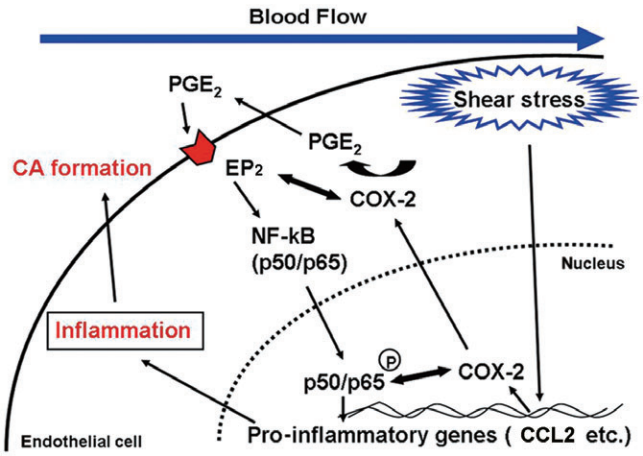

Figure 5
A proposed model for the formation of cerebral aneurysm induced by shear stress.

that suppress PG synthesis tended to suppress cerebral aneurysm rupture in four out of 49 cases (8.2%) in the subarachnoid haemorrhage group of NSAID users, whereas 26 out of 149 cases (17.4%) in the unruptured cerebral aneurysm group are NSAID users (chi-square test, $P = 0.11$). Although the findings from the case-control study suggest a potential of COX inhibitors as therapeutic agents for cerebral aneurysm, selective COX-2 inhibition produces a relative increase of TXA_2 over PGI_2 levels *in vivo* and increases the risk of cardiovascular events (Mukherjee *et al*. 2001; Juni *et al*., 2004; Funk and FitzGerald, 2007). EP_2 antagonism could thus circumvent this cardiovascular risk of COX-2 inhibition and could be a better pharmaceutical target for the medical treatment of cerebral aneurysm. This idea is reinforced by our findings that EP_2 expression was detected in SMC in the walls of advanced cerebral aneurysms. Thus, EP_2 antagonism could be useful not only in the prevention of cerebral aneurysm but also in the attenuation of the progression of cerebral aneurysms.

In summary, results from the present study suggest that shear stress activated the PGE_2-EP_2 pathway in ECs at the early stage of cerebral aneurysm formation and triggered chronic inflammation in arterial walls leading to cerebral aneurysm formation. This seems to occur through an amplification loop via NF-κB. In addition, given that selective COX-2 inhibitors carry the risk of cardiovascular events, our findings provide a possible alternative of EP_2 antagonists as a new class of drug against cerebral aneurysm.

Acknowledgements

This work was supported by Grants-in-Aid for Scientific Research from the Ministry of Education, Culture, Sports, Science and Technology of Japan and a collaborative grant to Kyoto University from ONO Pharmaceuticals (S.N.). T.A. is a recipient of the Research Fellowship for Young Scientists from Japan Society for the Promotion of Science. We thank Pfizer and Ono Pharmaceuticals for their kind gifts of celecoxib and EP agonists, respectively.

Conflicts of interest

The authors declare that the research by S.N. is supported in part by a collaborative grant to Kyoto University from Ono Pharmaceuticals, which also supports partially the mouse colonies and has provided several compounds used in this study.

References

Alexander SPH, Mathie A, Peters JA (2009). Guide to receptors and channels (GRAC), 4th edition (2009). Br J Pharmacol 158 (Suppl. 1): S1–S254.

Alnaes MS, Isaksen J, Mardal KA, Romner B, Morgan MK, Ingebrigtsen T (2007). Computation of hemodynamics in the circle of Willis. Stroke 38: 2500–2505.

Aoki T, Nishimura M (2010). Targeting chronic inflammation in cerebral aneurysms: focusing on NF-κB as a putative target of medical therapy. Expert Opin Ther Targets 14: 265–273.

Aoki T, Kataoka H, Morimoto M, Nozaki K, Hashimoto N (2007a). Macrophage-derived matrix metalloproteinase-2 and -9 promote the progression of cerebral aneurysms in rats. Stroke 38: 162–169.

Aoki T, Kataoka H, Shimamura M, Nakagami H, Wakayama K, Moriwaki T *et al*. (2007b). NF-κB is a key mediator of cerebral aneurysm formation. Circulation 116: 2830–2840.

Aoki T, Kataoka H, Ishibashi R, Nozaki K, Hashimoto N (2008a). Gene expression profile of the intima and media of experimentally induced cerebral aneurysms in rats by laser-microdissection and microarray techniques. Int J Mol Med 22: 595–603.

Aoki T, Kataoka H, Ishibashi R, Nozaki K, Hashimoto N (2008b). Simvastatin suppresses the progression of experimentally induced cerebral aneurysms in rats. Stroke 39: 1276–1285.

Aoki T, Moriwaki T, Takagi Y, Kataoka H, Yang J, Nozaki K *et al*. (2008c). The efficacy of apolipoprotein E deficiency in cerebral aneurysm formation. Int J Mol Med 21: 453–459.

Aoki T, Kataoka H, Ishibashi R, Nakagami H, Nozaki K, Morishita R *et al*. (2009a). Pitavastatin suppresses formation and progression of cerebral aneurysms through inhibition of the nuclear factor κB pathway. Neurosurgery 64: 357–365.

Aoki T, Kataoka H, Ishibashi R, Nozaki K, Egashira K, Hashimoto N (2009b). Impact of monocyte chemoattractant protein-1 deficiency on cerebral aneurysm formation. Stroke 40: 942–951.

Bayston T, Ramessur S, Reise J, Jones KG, Powell JT (2003). Prostaglandin E_2 receptors in abdominal aortic aneurysm and human aortic smooth muscle cells. J Vasc Surg 38: 354–359.

Breyer RM, Bagdassarian CK, Myers SA, Breyer MD (2001). Prostanoid receptors: subtypes and signaling. Annu Rev Pharmacol Toxicol 41: 661–690.

Chyatte D, Bruno G, Desai S, Todor DR (1999). Inflammation and intracranial aneurysms. Neurosurgery 45: 1137–1146.

Cornuz J, Sidoti PC, Tevaearai H, Egger M (2004). Risk factors for asymptomatic abdominal aortic aneurysm: systematic review and meta-analysis of population-based screening studies. Eur J Public Health 14: 343–349.

Everts B, Wahrborg P, Hedner T (2000). COX-2-Specific inhibitors – the emergence of a new class of analgesic and anti-inflammatory drugs. Clin Rheumatol 19: 331–343.

Feigin VL, Rinkel GJ, Lawes CM, Algra A, Bennett DA, van Gijn J *et al*. (2005). Risk factors for subarachnoid hemorrhage: an updated systematic review of epidemiological studies. Stroke 36: 2773–2780.

Fukuda S, Hashimoto N, Naritomi H, Nagata I, Nozaki K, Kondo S *et al*. (2000). Prevention of rat cerebral aneurysm formation by inhibition of nitric oxide synthase. Circulation 101: 2532–2538.

Funk CD, FitzGerald GA (2007). COX-2 inhibitors and cardiovascular risk. J Cardiovasc Pharmacol 50: 470–479.

van Gijn J, Kerr RS, Rinkel GJ (2007). Subarachnoid haemorrhage. Lancet 369: 306–318.

Hashimoto N, Handa H, Hazama F (1978). Experimentally induced cerebral aneurysms in rats. Surg Neurol 10: 3–8.

Hashimoto N, Handa H, Nagata I, Hazama F (1980). Experimentally induced cerebral aneurysms in rats: part V. Relation of hemodynamics in the circle of Willis to formation of aneurysms. Surg Neurol 13: 41–45.

Holmes DR, Wester W, Thompson RW, Reilly JM (1997). Prostaglandin E_2 synthesis and cyclooxygenase expression in abdominal aortic aneurysms. J Vasc Surg 25: 810–815.

Inoue H, Tada Y, Miwa Y, Yokota C, Miyagi M, Sasaguri T (2002). Transcriptional and posttranscriptional regulation of cycloocygenase-2 expression by fluid shear stress in vascular endothelial cells. Arterioscler Thromb Vasc Biol 22: 1415–1420.

Ishibashi R, Aoki T, Nishimura M, Hashimoto N, Miyamoto S (2010). Contribution of mast cells to cerebral aneurysm formation. Curr Neurovasc Res 7: 113–124.

Jayaraman T, Berenstein V, Li X, Mayer J, Silane M, Shin YS *et al*. (2005). Tumor necrosis factor alpha is a key modulator of inflammation in cerebral aneurysms. Neurosurgery 57: 558–564.

Juni P, Nartey L, Reichenbach S, Sterchi R, Dieppe PA, Egger M (2004). Risk of cardiovascular events and rofecoxib: cumulative meta-analysis. Lancet 364: 2021–2029.

King VL, Trivedi DB, Gitlin JM, Loftin CD (2006). Selective cyclooxygenase-2 inhibition with celecoxib decreases angiotensin II-induced abdominal aortic aneurysm formation in mice. Arterioscler Thromb Vasc Biol 26: 1137–1143.

Kobayashi T, Narumiya S (2002). Function of prostanoid receptors: studies on knockout mice. Prostaglandins Other Lipid Mediat 68–69: 557–573.

Kobayashi T, Tahara Y, Matsumoto M, Iguchi M, Sano H, Murayama T *et al*. (2004). Roles of thromboxane A_2 and prostacyclin in the development of atherosclerosis in apoE-deficient mice. J Clin Invest 114: 784–794.

Liao JK, Laufs U (2005). Pleiotropic effects of statins. Annu Rev Pharmacol Toxicol 45: 89–118.

Linn FH, Rinkel GE, Algra A, van Gijn J (1996). Incidence of subarachnoid hemorrhage. Stroke 27: 625–629.

Meng H, Wang Z, Hoi Y, Gao L, Metaxa E, Swartz DD *et al*. (2007). Complex hemodynamics at the apex of an arterial bifurcation induces vascular remodeling resembling cerebral aneurysm initiation. Stroke 38: 1924–1931.

Miralles M, Wester W, Sicard GA, Thompson R, Reilly JM (1999). Indomethacin inhibits expansion of experimental aortic aneurysms via inhibition of the cox2 isoform of cyclooxygenase. J Vasc Surg 29: 884–892.

Morimoto M, Miyamoto S, Mizoguchi A, Kume N, Kita T, Hashimoto N (2002). Mouse model of cerebral aneurysm: experimental induction by renal hypertension and local hemodynamic changes. Stroke 33: 1911–1915.

Morishita R, Tomita N, Kaneda Y, Ogihara T (2004). Molecular therapy to inhibit NFκB activation by transcription factor decoy oligonucleotides. Curr Opin Pharmacol 4: 139–146.

Moriwaki T, Takagi Y, Sadamasa N, Aoki T, Nozaki K, Hashimoto N (2006). Impaired progression of cerebral aneurysms in interleukin-1β-deficient mice. Stroke 37: 900–905.

Mukherjee D, Nissen SE, Topol EJ (2001). Risk of cardiovascular events associated with selective COX-2 inhibitors. JAMA 286: 954–959.

Murakami M, Nakatani Y, Tanioka T, Kudo I (2002). Prostaglandin E synthase. Prostaglandins Other Lipid Mediat 68-69: 383–399.

Nakatani H, Hashimoto N, Kang Y, Yamazoe N, Kikuchi H, Yamaguchi S *et al*. (1991). Cerebral blood flow patterns at major vessel bifurcations and aneurysms in rats. J Neurosurg 74: 258–262.

Narumiya S, Sugimoto Y, Ushikubi F (1999). Prostanoid receptors: structures, properties, and functions. Physiol Rev 79: 1193–1226.

Ogasawara A, Arakawa T, Kaneda T, Takuma T, Sato T, Kaneko H *et al*. (2001). Fluid shear stress-induced cyclooxygenase-2 expression is mediated by C/EBP β, cAMP-response element-binding protein, and AP-1 in osteoblastic MC3T3-E1 cells. J Biol Chem 276: 7048–7054.

Sadamasa N, Nozaki K, Hashimoto N (2003). Disruption of gene for inducible nitric oxide synthase reduces progression of cerebral aneurysms. Stroke 34: 2980–2984.

Schmedtje JF Jr, Ji YS, Liu WL, DuBois RN, Runge MS (1997). Hypoxia induces cyclooxygenase-2 via the NF-κB p65 transcription factor in human vascular endothelial cells. J Biol Chem 272: 601–608.

Sonoshita M, Takaku K, Sasaki N, Sugimoto Y, Ushikubi F, Narumiya S *et al*. (2001). Acceleration of intestinal polyposis through prostaglandin receptor EP_2 in $Apc^{\Delta 716}$ knockout mice. Nat Med 7: 1048–1051.

Sugimoto Y, Narumiya S (2007). Prostaglandin E receptors. J Biol Chem 282: 11613–11617.

Takagi Y, Ishikawa M, Nozaki K, Yoshimura S, Hashimoto N (2002). Increased expression of phosphorylated c-Jun amino-terminal kinase and phosphorylated c-Jun in human cerebral aneurysms: role of the c-Jun amino-terminal kinase/c-Jun pathway in apoptosis of vascular walls. Neurosurgery 51: 997–1002.

Takeuchi S, Karino T (2009). Flow patterns and distributions of fluid velocity and wall shear stress in the human internal carotid and middle cerebral arteries. Surg Neurol 73: 174–185.

Tilley SL, Coffman TM, Koller BH (2001). Mixed messages: modulation of inflammation and immune responses by prostaglandins and thromboxanes. J Clin Invest 108: 15–23.

Topper JN, Cai J, Falb D, Gimbrone MA Jr (1996). Identification of vascular endothelial genes differentially responsive to fluid mechanical stimuli: cyclooxygenase-2, manganese superoxide dismutase, and endothelial cell nitric oxide synthase are selectively up-regulated by steady laminar shear stress. Proc Natl Acad Sci USA 93: 10417–10422.

Wiebers DO, Whisnant JP, Huston J, III, Meissner I, Brown RD, Jr, Piepgras DG *et al*. (2003). Unruptured intracranial aneurysms: natural history, clinical outcome, and risks of surgical and endovascular treatment. Lancet 362: 103–110.

Yamamoto K, Sokabe T, Matsumoto T, Yoshimura K, Shibata M, Ohura N *et al*. (2006). Impaired flow-dependent control of vascular tone and remodeling in P2X4-deficient mice. Nat Med 12: 133–137.

Supporting information

Additional Supporting Information may be found in the online version of this article:

Figure S1 Characterization of primary culture of endothelial cells from human carotid artery and morphological change and COX-2 induction upon shear stress in these cells. (A) A phase-contrast image of cultured endothelial cells. Cells showed the cobblestone-like appearance, which was a character of endothelial cells. Bar = 300 μm. (B) Western blot analysis of cultured endothelial cells (ECs) from human carotid artery and cell lines derived from endothelial cells (aortic EC) and smooth muscle cells (aortic SMC). α-smooth muscle actin (SMA), a marker for smooth muscle cells, and von Willebrand Factor (vWF), a marker for endothelial cells were analysed. α-Tubulin was served as an internal control. (C) Immunostaining for VE-Cadherin (CD144), a marker for endothelial cells. Bar = 50 μm. (D) Uptake of FITC-labeled acetyl-LDL. Cells were incubated with FITC-labeled acetyl-LDL for 4 h. Bar = 50 μm. The above data verified the endothelial profile of these primary cells. (E) Phase-contrast images of endothelial cells without (0 Pa) or with (1.5 Pa) shear stress. An arrow shows the direction of shear stress. Cells were stretched upon shear stress, compared with a cobblestone-like appearance without shear stress. Bar = 100 μm. (F) Immunostaining for COX-2 (green) without or with shear stress. DAPI was used for nuclear staining (blue). Shear stress induced COX-2 expression in endothelial cells.

Figure S2 Characterization of COX-2 and EP_2 expressing cells in human CA walls. (A) Double immunostaining for COX-2 (black) with either von Willebrand factor (vWF, red), a marker for endothelial cells, or α- smooth muscle actin (SMA, red), a marker for smooth muscle cells. (B) Double immunostaining for EP_2 (black) with the same markers as in (A). Bar = 20 μm. Note that COX-2 and EP_2 were expressed in both endothelial cells and smooth muscle cells.

Figure S3 Induction of COX-2 and mPGES1 in rat CA walls and characterization of COX-2 expressing cells. (A) Immunostaining for either COX-2 or COX-1 (green) with a-smooth muscle actin (red), a marker for smooth muscle cells, before (0 M) and at 3 months after (3 M) CA induction. Adjacent sections stained by Elastica van Gieson staining (EvG) are also shown. Representative images (right) were taken from an area indicated by the box in the schema of the arterial bifurcation (left). COX-2 expression was induced during CA formation, while COX-1 expression was not altered. Bar = 20 μm. ACA: anterior cerebral artery, ICA: internal carotid artery, OA: olfactory artery. (B) Double immunostaining for COX-2 (green) and either CD68 (for macrophage, red), endothelial nitric oxide synthase (eNOS for endothelial cells, red) or α-smooth muscle actin (SMA for smooth muscle cells, red). COX-2 was expressed in all the examined cell types, especially in macrophages and endothelial cells. Bar = 20 μm. (C) Proportions of CD68-positive, eNOS-positive or SMA-positive cells in COX-2 expressing cells (n = 5). Data were analysed using Kruskal–Wallis test followed by *post hoc* Dunn's test. $^*P < 0.05$. (D) Immunostaining for mPGES1, mPGES2 or cPGES at the arterial bifurcation before (0 M) and at 3 months after (3 M) CA induction. Whereas these isoforms were constitutively expressed in this region, mPGES1, but not cPGES nor mPGES2, was up-regulated during CA formation. Note that mPGES1 induction was most prominent at the neck portion of CA (arrows). Bar = 50 μm.

Figure S4 Western blot analysis and immunostaining for EP_2 expression during CA formation. (A) Western blot analysis for EP_2. Proteins were extracted from the circle of Willis of rats before (0 M) and at 1 month (1 M) and 3 months after (3 M) CA induction and subjected to Western blot analysis (left). A representative blot from 5 independent experiments is shown. EP_2 was induced in cerebral arteries during CA formation. The specificity of EP_2 antibody was confirmed using samples from wild-type (*Ptger2*$^{+/+}$) and *Ptger2*-deficient mice (*Ptger2*$^{-/-}$) (right). α-Tubulin was served as an internal control. (B) Immunostaining for EP_2. EP_2 (green) and α-smooth muscle actin (red), a marker for smooth muscle cells, were stained at the arterial bifurcation before (0 M) and at 1 month (1 M) and 3 months after (3 M) CA induction (left). Bar = 20 μm. EP_2 signals were increased during CA formation. EP_2 signals were abolished in the tissue from *Ptger2*-deficient mice (*Ptger2*$^{-/-}$), confirming the specificity of EP_2 antibody (right). Bar = 10 μm.

Figure S5 The architecture of the circle of Willis and systemic blood pressure after CA induction in *Ptger2*-deficient mice. (A) The architecture of the circle of Willis from wild-type (*Ptger2*$^{+/+}$) and *Ptger2*-deficient mice (*Ptger2*$^{-/-}$). No apparent difference was observed between the two genotypes. MCA: middle cerebral artery. Other abbreviations are the same as in Supporting Information Figure S3. (B) The systemic blood pressure (systolic blood pressure) of mice deficient of each EP subtypes (*Ptger1*$^{-/-}$, *Ptger2*$^{-/-}$, *Ptger3*$^{-/-}$, *Ptger4*$^{-/-}$), *Ptger2*-heterozygous mice (*Ptger2*$^{+/-}$), and wild-type mice (WT) at 5 months after CA induction. Systemic blood pressure was similar across the genotypes. Numbers of animals are shown in parentheses. Data were analysed using Kruskal–Wallis test followed by *post hoc* Dunn's test. $^*P < 0.05$ compared with the value of wild-type mice.

Figure S6 The contents of PGI_2 and thromboxane A_2 metabolites in CA walls and the incidence of CA formation in mice deficient in either *Tbxa2r* or *Ptgir*. (A) The contents of 6-keto-$PGF_{1\alpha}$ and TxB_2, stable metabolites of PGI_2 and TXA_2, respectively, in the arterial bifurcation before (0 M) and at 1 month (1 M) and 3 months after (3 M) CA induction. The content was measure by ELISA and normalized to the wet weight of tissues. The contents of these metabolites were also measured in rats at 3 months after sham operation (sham). Data were analysed using Kruskal–Wallis test followed by *post hoc* Dunn's test (n = 5). $^*P < 0.05$, $^{**}P < 0.01$. (B) The incidence of CA formation in mice deficient either *Tbxa2r* (*Tbxa2r*$^{-/-}$) or *Ptgir* (*Ptgir*$^{-/-}$) and wild-type mice (WT). No significant difference was observed in *Tbxa2r*$^{-/-}$ *or Ptgir*$^{-/-}$ mice compared to wildtype mice. Numbers of animals are shown in parentheses. Incidence was analysed by Fisher's exact test.

Figure S7 Effects of celecoxib treatment on chronic inflammation in CA walls. (A) Systemic blood pressure (systolic blood pressure) of rats treated with celecoxib. Rats were treated with celecoxib or vehicle at 150 $mg \cdot kg^{-1} \cdot day^{-1}$ for 3 months after CA induction. The systemic blood pressure was measured by the tail-cuff method. Numbers of animals are shown in the parentheses. Data were analysed using Mann–Whitney *U*-test. (B) The number of CD68-positive macrophages in CA walls. CD68-positive macrophages were identified by immunostaining. Numbers of animals are shown in parentheses below each bar. Celecoxib treatment significantly inhibited macrophage infiltration in CA walls. Data were analysed using Mann–Whitney *U*-test. $*P < 0.05$. (C) Effects of celecoxib on mRNA levels of *Mmp2*, *Ccl2* and *Il-1β* at the arterial bifurcation before (0 M) and after (3 M) CA induction. mRNA levels were determined by quantitative RT-PCR analysis ($n = 6$). Data were analysed using Kruskal–Wallis test followed by *post hoc* Dunn's test. $*P < 0.05$, $**P < 0.01$. (D) Immunostaining for MMP2, CCL2 and IL-1β in CA walls of rats treated without or with celecoxib. Green signals show MMP2, CCL2 or IL-1β in the corresponding images. Red signals show the signal for α-smooth muscle actin. Bar = 20 μm. (E) The effect of celecoxib treatment on gelatinase activity of MMP2 in cerebral arteries of rats during CA formation. Cerebral arteries from sham-operated rats (sham) or CA-induced rats without or with celecoxib treatment were subjected to gelatin zymography. A representative image (upper) and average signal intensities of MMP2 band from five independent experiments (lower) are shown. Data were analysed using Kruskal–Wallis test followed by *post hoc* Dunn's test. $*P < 0.05$, $**P < 0.01$. (F) The effect of celecoxib on NF-κB phosphorylation. The phosphorylated form of NF-κB p65 was immunostained in CA walls without or with celecoxib (left), and the proportion of positive cells was quantified (right) ($n = 5$). DAPI was used for nuclear staining (blue). Data were analysed using Mann–Whitney *U*-test. $**P < 0.01$. Celecoxib treatment significantly suppressed NF-κB activation. (G) Immunostaining for COX-2 and the phosphorylated form of NF-κB p65 subunit (p-p65) in rat CA walls at 3 months after CA induction. These two signals were mostly co-localized. Bar = 20 μm. (H) The effect of NF-κB decoy ODN on COX-2 expression in CA wall. Rats were treated with NF-κB decoy ODN and scrambled decoy ODN for 3 months after CA induction. COX-2 and the α-smooth muscle actin are shown in green and red, respectively. Bar = 30 μm. NF-κB inactivation by its decoy ODN suppressed COX-2 expression.

Figure S8 The effect of an EP receptor agonist on NF-κB phosphorylation and CCL2 expression and EP_2 knockdown by RNAi in endothelial cells from human carotid artery. (A) Western blot analysis for the phosphorylated form of NF-κB p65 subunit (p-p65) and CCL2 expression in endothelial cells treated with 16-16-dimethyl PGE_2, an EP receptor agonist, or vehicle for 24 h. Representative blots from 5 independent experiments are shown. α-Tubulin was served as an internal control. (B) The quantification by the densitometric analysis for NF-κB phosphorylation (p-p65, left) and CCL2 (right) ($n = 5$). This EP agonist induced NF-κB phosphorylation and CCL2 expression in a dose-dependent manner. Data were analysed using Kruskal–Wallis test followed by *post hoc* Dunn's test. $*P < 0.05$, $**P < 0.01$. (C) Western blot analysis (left) and immunostaining (right) for EP_2 in primary culture of endothelial cells. Bar = 50 μm. (D, E) EP_2 depletion by RNAi. Cells were transfected with scrambled (control) or human *Ptger2* siRNA and incubated for 72 h. Quantitative RT-PCR analysis (D, $n = 6$) and Western blot analysis (E, $n = 5$) were performed. α-Tubulin was served as an internal control. Data were analysed using Mann–Whitney *U*-test. $*P < 0.05$, $**P < 0.01$.

Figure S9 Induction of *iNos* and *Il-1β* mRNA by an EP_2 agonist in the primary culture of smooth muscle cells. (A) Induction of *iNos* and *Il-1β* mRNA by EP agonists. Primary culture of smooth muscle cells was incubated with agonists selective to each EP subtypes (EP_1 to EP_4) at 0.5 μM and vehicle for 24 h. mRNA levels were determined by quantitative RT-PCR analysis ($n = 6$). Only an EP_2 agonist induced *iNos* and *Il-1β* mRNA expression. Data were analysed using Kruskal–Wallis test followed by *post hoc* Dunn's test. $*P < 0.05$, $**P < 0.01$. (B) A dose-dependent effect of an EP_2 agonist on *iNos* and *Il-1β* mRNA expression ($n = 6$). Data were analysed using Kruskal–Wallis test followed by *post hoc* Dunn's test. $*P < 0.05$, $**P < 0.01$.